

Activated protein phosphatase 2A disrupts nutrient sensing balance between mTORC1 and AMPK causing sarcopenia in alcoholic liver disease

Gangarao Davuluri¹, Nicole Welch^{1,4}, Jinendiran Sekar¹, Mahesha Gangadhariah¹, Khaled Alsabbagh Alchirazi¹, Maradumane L Mohan², Avinash Kumar¹, Sashi Kant¹, Samjhana Thapaliya¹, McKenzie Stine¹, Megan R McMullen¹, Rebecca L. McCullough¹, George R. Stark³, Laura E. Nagy¹, Sathyamangla V Naga Prasad^{2*}, Srinivasan Dasarathy^{1,4*}. Departments of ¹Inflammation and Immunity, ²Cardiovascular and Metabolic Sciences, ³Cancer Biology and ⁴Gastroenterology and Hepatology, Cleveland Clinic, Cleveland, OH.

Table of contents.

- 1. Supplementary methods**
- 2. Supplementary Tables**
- 3. Supplementary figure legends**
- 4. Supplementary figures**
- 5. References**

Supplementary Methods Section.

Antibodies: Antibodies against the following components were used: puromycin, methylated and phosphorylated PP2A, the catalytic subunit of PP2A, PP2A- B56 (EMD Millipore, Burlington, MA), LC3B (Novus Biologicals, Littleton, CO), SQSTM1/p62 (R&D Systems, Inc., Minneapolis, MN 55413), and ACTB/ β -actin, PI3K γ , I1 and I2PP2A (Santa Cruz Biotechnology Inc., Dallas, TX). Antibodies against ATG7, BECN1/Beclin1, total and phosphorylated 4E binding protein 1, Akt, AMP kinase, ERK, JNK1, MAPK p38, mTORC1, P70S6 kinase, ribosomal S6 protein, total and phosphorylated ULK1 (Ser^{317, 555, 757, 777}) and TSC2 (Ser¹³⁸⁷) were obtained from Cell Signaling Technologies (Danvers, MA). Catalog numbers for antibodies are provided in Supplementary Table 1. All other chemicals used in this study were obtained from Sigma Aldrich (St. Louis, MO) unless specified.

Generation of phospho-I2PP2A antibody. Polyclonal antibody against phosphorylated form of I2PP2A was generated in the Cleveland Clinic Hybridoma Core facility by immunizing rabbits with a synthetic peptide corresponding to residues surrounding Ser9 of human I2PP2A (APAAKCpSKKELNC). The serum was collected and tested by immunoblotting in vitro phosphorylated bacterial purified I2PP2A. The polyclonal antibody recognizes phospho-I2PP2A with high fidelity.

Mouse studies. The Cleveland Clinic Institutional Animal Care and Use Committee approved all procedures using mice. 12-week-old female C57BL/6 mice with and without knockout of PI3K γ were allowed free access to a Lieber DeCarli liquid diet (Dyets Inc., 710260) containing ethanol (n=10 each) or isocalorically substituted maltodextrins (n=8 each). To quantify autophagy flux *in vivo*, mice (n=4 in pair fed and n=5 in ethanol fed in each group) were injected with colchicine intraperitoneally daily for 3 days at a dose of 0.4 mg/kg. Data on this subgroup was presented separately for autophagy flux *in vivo* and compared with the data from mice that were injected saline instead of colchicine and the responses were similar in the 2 groups (**Supplementary Table 2**). Subsequently, critical experiments were repeated in 12 week old male C57/BL6 mice with and without PI3K γ knockout to determine if there were gender specific differences. In brief, mice were acclimatized with a liquid diet for 2 days, and ethanol was added to the liquid diet and mice were administered ethanol as follows: 1% ethanol for 2 days, 2% ethanol for 2 days, 4% ethanol for 7 days, 5% ethanol for 7 days, and then 6% ethanol for 7 days. On the study day, mice were euthanized by anesthesia using a 0.1 ml/25 g body weight rodent cocktail (60 mg/kg ketamine, 12 mg/kg xylazine, 2 mg/kg acepromazine) followed by laparotomy and

exsanguination of blood from the inferior vena cava. Gastrocnemius and tibialis anterior muscle were harvested rapidly, blotted dry, weighed and flash frozen in liquid nitrogen and stored at -80 °C for subsequent assays. We have previously reported that mice fed ethanol using this protocol do not show evidence of muscle injury or necrosis on histology⁽¹⁾. Animals were killed and tissues harvested between 9AM and 11AM to avoid circadian differences in responses.

PI3K γ knockout. The PI3K γ -deficient mice were a gift from Dr. Diangng Wu from the University of Connecticut and have been bred in the Cleveland Clinic Biological Resource Unit⁽²⁻⁵⁾. In brief, a mouse line was generated by transfection into embryonic stem cells, an 8-kb genomic DNA isolated from a mouse 129sv genomic DNA library containing at least the first three exons of mouse PI3K γ . A part of the first and the entire second and third exons were replaced by cDNA encoding GFP, which was then fused in frame with the coding sequence of PI3K γ . A neomycin-resistant gene expression unit was inserted behind GFP to select transfected embryonic stem (ES) cells. Three positive ES clones were used to produce chimeras. Mice heterozygous and homozygous for the disrupted PI3K γ genes were generated by standard breeding protocols. The details of these procedures are described in the original publications by Dr. Li et al and our previous publications⁽²⁻⁵⁾.

In vitro cell culture studies. C2C12 murine myoblasts (ATCC; CRL 1772, Manassas, VA) at 3-4 passage were grown to confluence in proliferation medium (Dulbecco's modified Eagle medium (DMEM) containing 10% fetal bovine serum) followed by differentiation in DMEM with 2% horse serum for 48 h as previously described⁽⁶⁾. Myotubes were then exposed to 100 mM ethanol for varying times. Ethanol-treated and control cells were harvested at the same times. The concentration and time of exposure of myotubes to ethanol in these studies were determined based on the ability to reproduce the molecular responses in the skeletal muscle of human patients and ethanol fed mice and not on circulating concentrations of ethanol in these in vivo models. Myotubes were treated with 5 nM fostriecin that is highly specific for PP2A inhibition⁽⁷⁻⁹⁾. Ethanol toxicity was evaluated by cell viability using trypan blue exclusion⁽¹⁰⁾.

Stable transfection of constructs. Sub-confluent myoblasts were transfected with wild type, myristoylated, or kinase-dead variants of PI3K γ , or shRNA corresponding to the catalytic subunit of PP2A, using the Transfect®

reagent per the manufacturer's protocol (Mirus biological Inc., Madison, WI). Stably transfected cells were selected using puromycin for the shPP2A cell line and neomycin (G418) for the PI3Ky cell lines at concentrations of 20 µg/ml and 400 µg/ml in the medium, respectively. Transfection efficiencies were confirmed by immunoblot assays.

Protein synthesis. In vitro. Rates of protein synthesis were quantified by incorporation of puromycin, as previously reported⁽¹¹⁾. The puromycin incorporation method to quantify protein synthesis is based on the principle that puromycin is incorporated into elongating proteins thereby terminating the translation of proteins. The puromycin incorporation into the newly synthesized proteins at the N-terminal can be detected by using a monoclonal anti-puromycin antibody. In the context of our studies, this method is used to quantify synthesis (or lack thereof) of proteins by densitometry quantification of all the bands in the entire lane.

In brief, myotubes were treated with 100 mM ethanol for varying times and, during the last 30 min, 2 µg/ml puromycin was added to the medium. At the end of the study, cells were washed in ice-cold PBS, lysed with RIPA buffer (25 mM Tris•HCl pH 7.6, 150 mM NaCl, 1% NP-40, 1% sodium deoxycholate, 0.1% SDS) + protease and phosphatase inhibitors (Sigma Aldrich, St Louis, MO), protein was extracted, quantified and immunoblotted for puromycin incorporation. Densitometry was done for all bands in the lane as a measure of global protein synthesis. In cell lines with stable transfection of shPP2A, incorporation of ³H phenylalanine was determined, as previously described, because puromycin was used for selection and could not be used for quantifying protein synthesis⁽¹¹⁾. In brief, following incubation for 6 h in 100 mM ethanol, the cells were washed with sterile phosphate-buffered saline, and 1 µCi of ³H-labeled phenylalanine was added to each well. After 30 min, the cells were washed, lysed with RIPA buffer, and the incorporation of ³H phenylalanine was quantified in solubilized, precipitated protein, using a Beckman scintillation counter (Perkin Elmer, Waltham, MA), and the data were normalized to cellular protein content.

In vivo. On the study day, a flooding dose of D₅-phenylalanine was injected intraperitoneally 30 min before euthanasia using methods previously described by us^(12, 13). After euthanasia, a part of the frozen gastrocnemius muscle was used to quantify the fractional and total muscle synthesis rates as previously described⁽¹²⁾. In addition to the fractional synthesis rate, we also measured the total muscle synthesis rate to avoid the effect of the reduction in muscle mass in ethanol fed mice.

Sample preparation and derivatization. The rate of muscle protein synthesis was estimated by measuring the free and protein-bound [D_5]-phenylalanine (tracer to trace ratio) in muscle samples from the gastrocnemius muscle as previously reported with minor modifications⁽¹²⁾. Frozen muscle samples (25-40 mg) were precisely weighed, homogenized in 0.5 ml of ice-cold 14% perchloric acid using a probe sonicator for one minute, followed by centrifugation at 10,000 g for 15 min at 4°C. The supernatant was collected and this process was repeated two more times, with all supernatants combined as the cytosolic fraction (free phenylalanine). The pellet was washed once in MilliQ water and three times in 100% ethanol. Each wash was followed by centrifugation at 10,000 g for 15 min at 4°C. The pellet with the bound muscle proteins was dried overnight at 50°C and hydrolyzed in 2 ml of 6N hydrochloric acid (HCl) for 24 h at 100 °C. The free and protein-bound hydrolysates were washed over a cation exchange column (Dowex AG 50W-8X, 200-400 mesh, H⁺ form, Sigma). Amino acids were eluted from the column with 4N ammonium hydroxide and the eluate was collected and dried under vacuum. The dried samples were derivatized with 80 μ l of N-tert-Butyldimethylsilyl-N-methyltrifluoroacetamide with 1% tert-Butyldimethylchlorosilane (MTBSTFA with 1% TBDMS; Restek, Bellefonte, PA) at 80°C for 4 h. After incubation, samples were centrifuged at 10,000g for 10 min and the sample (65 μ l) was transferred into a GC vial for analysis.

Stable isotope tracer analysis. All samples were analyzed by using Agilent gas chromatography-mass spectrometry (GC-MS) coupled with electron impact ionization (Agilent Technologies; Santa Clara, CA). For [2H_5]-phenylalanine, m/z 234 (m+0), 235 (m+1), 237 (m+3), and 239 (m+5) were monitored, with m+0 representing the lowest molecular weight of the ion (**Supplementary Fig. 7,C**). The fractional synthesis rate (FSR) was calculated as the rate of [2H_5]-phenylalanine tracer incorporated into muscle protein using the formula: $FSR (\%) = S_B \times 100 / S_A \times t$, where, S_B is the protein bound-phenylalanine, S_A is the free phenylalanine, and t is the incorporation time in hours. The synthesis rate in the entire muscle (total synthesis rate) was calculated as $FSR \times \text{muscle mass} / \text{mass of tissue used for analysis}$. These methods and calculations have been previously reported by us⁽¹²⁾.

Autophagy flux. In vitro. Autophagy flux was determined in vitro in differentiated myotubes treated with ethanol or medium with/without a lysosomal fusion inhibitor, chloroquine (10 μ M as previously reported by us^(1, 14)). In brief, following treatment, immunoblots for Beclin, LC3 and p62 were performed. In addition, myoblasts were

transfected with LC3-GFP construct, differentiated to myotubes and treated with ethanol or medium on glass slides with or without chloroquine. After 6h, cells were washed with phosphate buffered saline, fixed in paraformaldehyde, mounted and images acquired on a Leica TCS SP2 confocal laser scanning microscope. GFP-LC3B puncta were counted and expressed as number of cells with >5 green puncta per cell as described earlier^(1, 15). Puncta were scored on Z-stack overlays from at least 4 separate fields with ~100 nuclei and analyses performed using ImagePro.

In vivo. In vivo autophagy flux in mice was quantified following intraperitoneal administration of colchicine as detailed in the mice studies above and earlier⁽¹⁵⁾. LC3, Beclin1 and p62 expression were quantified on immunoblots of proteins from gastrocnemius muscle and densitometry performed.

Immunoblots. These assays were performed using our previously described protocols⁽¹⁵⁾. In brief, total muscle protein was extracted from a precisely weighed sample (~30 mg) of frozen skeletal muscle, or from cultured cells, with ice-cold RIPA buffer (Thermo Scientific, Waltham, MA) to which protease and phosphatase inhibitors (Sigma Aldrich, St Louis, MO) were added, and these samples were stored at -80 °C for subsequent assays. For immunoblots, equal amounts of protein samples were loaded into a 4-12% gradient gel, electrophoresed, and then electro-transferred onto PVDF membranes, incubated overnight at 4° C with primary antibodies, followed by incubation with appropriate secondary antibodies. The primary antibody dilutions were 1:1000 for all antibodies except SQSTM1 (1:500) and antipuromycin antibody (1:10,000). All secondary antibodies were used at a dilution of 1:15,000. Expression of β -actin was used as a loading control. Immune reactivity was detected by using a chemiluminescent horseradish peroxidase substrate (Millipore, Burlington, MA). Densitometry was done using Image J[®] software, as described earlier⁽¹⁵⁾. Due to proximity of bands of total and phosphorylated proteins in many instances and concerns with stripping to repeat the immunoblots, simultaneous gels with equal quantities of proteins were run in the same gel-box under identical conditions, electrotransferred to membranes under identical conditions. Subsequently, they were probed for total and phosphorylated proteins. For each blot, the appropriate β -actin blot was used for normalization and representative β -actin blots were shown for each panel.

Immunoprecipitation assays. To demonstrate the association of proteins, immunoprecipitations were performed using specific antibodies, followed by probing for associated proteins. Cells were harvested in lysis buffer containing 20 mM Tris pH 7.4, 137 mM NaCl, 1% NP-40, 1 mM PMSF, 20% glycerol, 10 mM sodium

fluoride, 1 mM sodium orthovanadate, 2 µg/ml leupeptin and aprotinin. The lysates were cleared by centrifugation at 12,000 g for 15 min at 4°C. The supernatant solutions were used for immunoprecipitation. Regulatory proteins (PI3K γ , PP2A, ULK1, Akt, mTOR, AMPK, I1 and I2 PP2A) were immunoprecipitated by incubating the cell lysates with protein A/G agarose beads (Santa Cruz biotechnology, Santa Cruz, CA) and respective antibodies at 1:500 dilutions, overnight at 4°C.

PP2A activity assay. We generated a threonine phosphopeptide, K-R-pT-I-R-R that is targeted by PP2A as a substrate. The phosphopeptide was synthesized by standard Fmoc solid-phase chemistry, using side chain-protected amino acids, including phospho-Tyr, on a Liberty Blue Automated Microwave Peptide Synthesizer (CEM Corporation, Matthews, NC) in the Cleveland Clinic Molecular Biotechnology Core. The peptide was purified to >95% purity by gradient elution (~20-25% acetonitrile) on a Vydac preparative C18 column, using reverse-phase HPLC (Waters Corporation). The quality of the peptide was assayed by analytical HPLC (Beckman System Gold) coupled with a reverse phase C-18 column. The correct mass (Mass: 909.35) corresponding to the amino acid composition of the phospho-peptide was confirmed by mass spectrometry (MALDI-TOF/TOF mass spectrometer; Model No. 4800; AB SCIEX, Framingham, MA). Following immunoprecipitation of PP2A from cell lysates, the protein was resuspended in phosphate-free buffer and incubated with the substrate for 10 min. Negative controls included reactions with no immunoprecipitate or phospho-threonine substrate. Acid malachite green solution was added and the optical density was read at 630 nM in a plate reader (Molecular Devices, Sunnyvale, CA).

PI3K γ activity assay. Thin layer chromatography was used to quantify PI3K γ activity in myotubes and in the skeletal muscles of mice, using methods previously described^(5, 16-19). Skeletal muscles were homogenized using a Polytron Homogenizer in 1.5 ml of lysis buffer (1% NP-40, 10% glycerol, 137 mM NaCl, 20 mM Tris-Cl (pH 7.4), 1 mM PMSF, 20 mM sodium fluoride, 1 mM sodium-pyrophosphate, 1mM sodium-orthovanadate and 2 µg/ml each of aprotinin and leupeptin) or C2C12 cells were lysed in lysis buffer and centrifuged at 38,000 X g for 25 min. 700 µg of clarified skeletal muscle extract or 500 µg of differentiated C2C12 myotube lysate was used for immunoprecipitation with PI3K γ (1:100) (Santa Cruz) along with 35 µl of protein G-agarose beads (ROCHE) by overnight toggling at 4°C. The samples were centrifuged at 10,000 rpm for 1 min and sedimented beads were washed once with lysis buffer, three times with phosphate buffered saline containing 1% NP40 and 100 µM sodium-orthovanadate, three times with 100 mM Tris-hydrochloride, pH 7.4, containing 5 mM LiCl and

100 μ M sodium-orthovanadate, and twice with TNE (10 mM Tris.Cl, pH 7.4, 150 mM NaCl, 5 mM EDTA, and 100 μ M sodium-orthovanadate). The last traces of buffer were completely removed using an insulin syringe and the pelleted beads were resuspended in 50 μ l of fresh TNE. To the resuspended pellet, 10 μ l of 100 mM magnesium chloride and 10 μ l of 2 mg/ml phosphatidyl inositol (PtdIns) (20 μ g) sonicated in TE (10 mM Tris HCl, pH 7.4, and 1 mM EDTA) were added.

Lipid (PtdIns) Preparation: PtdIns (Avanti) was dissolved in chloroform at a concentration of 10 mg/ml. 50 μ l of this stock was dried down in a stream of air in a 1.5-ml Eppendorf tube. 250 μ l of TE (Tris-EDTA) was added to the Eppendorf tube for a final concentration of 2 mg/ml. The lipids were suspended by sonicating them in an ice bath for 5–10 min. Sonicated lipids were then added to each reaction.

The reactions were started by adding 10 μ l of 440 μ M ATP, 10 μ Ci 32 p ATP, and were incubated at 23°C for 10 min with continuous agitation. The reactions were stopped with 20 μ l 6N HCl. Extraction of the lipids were done by adding 160 μ l of chloroform: methanol (1:1) and the samples were vortexed and centrifuged at room temperature to separate the phases. 30 μ l of the lower organic phase was spotted on to the 200- μ silica-coated flexi-thin layer chromatography (TLC) plates (Selecto-flexible; Fischer Scientific) and pre-coated with 1% potassium oxalate. The spots were allowed to dry and resolved chromatographically with 2N glacial acetic acid:1-propanol (1:1.87). The plates were dried after resolution, exposed for autoradiography. The densitometry analysis was performed by quantifying the density of the PIP generated following the lipid kinase activity. The measurement of the PIP provides a measure of PI3K γ activity associated with each of the samples.

Statistical analyses. All data were expressed as mean \pm SD unless specified. Qualitative variables were compared using the chi square test. Quantitative variables were compared by the Student's 't' test or for multiple group comparisons, analysis of variance with Bonferroni post-hoc analysis.

References.

1. Thapaliya S, Runkana A, McMullen MR, Nagy LE, McDonald C, Naga Prasad SV, Dasarathy S. Alcohol-induced autophagy contributes to loss in skeletal muscle mass. *Autophagy* 2014;10:677-690.
2. Li Z, Jiang H, Xie W, Zhang Z, Smrcka AV, Wu D. Roles of PLC-beta2 and -beta3 and PI3Kgamma in chemoattractant-mediated signal transduction. *Science* 2000;287:1046-1049.
3. Xie W, Samoriski GM, McLaughlin JP, Romoser VA, Smrcka A, Hinkle PM, Bidlack JM, et al. Genetic alteration of phospholipase C beta3 expression modulates behavioral and cellular responses to mu opioids. *Proc Natl Acad Sci U S A* 1999;96:10385-10390.
4. Mohan ML, Jha BK, Gupta MK, Vasudevan NT, Martelli EE, Mosinski JD, Naga Prasad SV. Phosphoinositide 3-kinase gamma inhibits cardiac GSK-3 independently of Akt. *Sci Signal* 2013;6:ra4.
5. Vasudevan NT, Mohan ML, Gupta MK, Hussain AK, Naga Prasad SV. Inhibition of protein phosphatase 2A activity by PI3Kgamma regulates beta-adrenergic receptor function. *Mol Cell* 2011;41:636-648.
6. Davuluri G, Allawy A, Thapaliya S, Rennison JH, Singh D, Kumar A, Sandler Y, et al. Hyperammonaemia-induced skeletal muscle mitochondrial dysfunction results in cataplerosis and oxidative stress. *J Physiol* 2016;594:7341-7360.
7. Swingle M, Ni L, Honkanen RE. Small-molecule inhibitors of ser/thr protein phosphatases: specificity, use and common forms of abuse. *Methods Mol Biol* 2007;365:23-38.
8. Walsh AH, Cheng A, Honkanen RE. Fostriecin, an antitumor antibiotic with inhibitory activity against serine/threonine protein phosphatases types 1 (PP1) and 2A (PP2A), is highly selective for PP2A. *FEBS Lett* 1997;416:230-234.
9. Armstrong SC, Kao R, Gao W, Shivell LC, Downey JM, Honkanen RE, Ganote CE. Comparison of in vitro preconditioning responses of isolated pig and rabbit cardiomyocytes: effects of a protein phosphatase inhibitor, fostriecin. *J Mol Cell Cardiol* 1997;29:3009-3024.
10. Strober W. Trypan Blue Exclusion Test of Cell Viability. *Curr Protoc Immunol* 2015;111:A3 B 1-A3 B 3.
11. Davuluri G, Krokowski D, Guan BJ, Kumar A, Thapaliya S, Singh D, Hatzoglou M, et al. Metabolic adaptation of skeletal muscle to hyperammonemia drives the beneficial effects of l-leucine in cirrhosis. *J Hepatol* 2016;65:929-937.

12. Dasarathy S, McCullough AJ, Muc S, Schneyer A, Bennett CD, Dodig M, Kalhan SC. Sarcopenia associated with portosystemic shunting is reversed by follistatin. *J Hepatol* 2011;54:915-921.
13. Tsien C, Davuluri G, Singh D, Allawy A, Ten Have GA, Thapaliya S, Schulze JM, et al. Metabolic and molecular responses to leucine-enriched branched chain amino acid supplementation in the skeletal muscle of alcoholic cirrhosis. *Hepatology* 2015;61:2018-2029.
14. Kumar A, Davuluri G, Welch N, Kim A, Gangadhariah M, Allawy A, Priyadarshini A, et al. Oxidative stress mediates ethanol-induced skeletal muscle mitochondrial dysfunction and dysregulated protein synthesis and autophagy. *Free Radic Biol Med* 2019;145:284-299.
15. Qiu J, Tsien C, Thapalaya S, Narayanan A, Weihl CC, Ching JK, Eghtesad B, et al. Hyperammonemia-mediated autophagy in skeletal muscle contributes to sarcopenia of cirrhosis. *Am J Physiol Endocrinol Metab* 2012;303:E983-993.
16. Naga Prasad SV, Esposito G, Mao L, Koch WJ, Rockman HA. Gbetagamma-dependent phosphoinositide 3-kinase activation in hearts with in vivo pressure overload hypertrophy. *J Biol Chem* 2000;275:4693-4698.
17. Naga Prasad SV, Laporte SA, Chamberlain D, Caron MG, Barak L, Rockman HA. Phosphoinositide 3-kinase regulates beta2-adrenergic receptor endocytosis by AP-2 recruitment to the receptor/beta-arrestin complex. *J Cell Biol* 2002;158:563-575.
18. Naga Prasad SV, Jayatilleke A, Madamanchi A, Rockman HA. Protein kinase activity of phosphoinositide 3-kinase regulates beta-adrenergic receptor endocytosis. *Nat Cell Biol* 2005;7:785-796.
19. Perrino C, Schroder JN, Lima B, Villamizar N, Nienaber JJ, Milano CA, Naga Prasad SV. Dynamic regulation of phosphoinositide 3-kinase-gamma activity and beta-adrenergic receptor trafficking in end-stage human heart failure. *Circulation* 2007;116:2571-2579.

Supplementary Table 1. Antibody List

Antibody name	Catalog No.	Company
Phospho AMPK α	2535S	Cell Signaling Technologies
AMPK α	2532S	Cell Signaling Technologies
Phospho AKT-Thr308	13038	Cell Signaling Technologies
Phospho AKT-Ser473	4060S	Cell Signaling Technologies
beta Actin	sc-47778	Santa Cruz Biotechnology
Beclin1	3495S	Cell Signaling Technologies
Phospho P70S6K	2708	Cell Signaling Technologies
P70S6K	9202	Cell Signaling Technologies
Phospho mTORC	5536S	Cell Signaling Technologies
mTORC	2972S	Cell Signaling Technologies
Phospho S6Ribosomal	4858S	Cell Signaling Technologies
S6Ribosomal	2217S	Cell Signaling Technologies
LC3-B	NB100-2220	Novus Biologicals
Phospho 4E-BP1	9456S	Cell Signaling Technologies
4E-BP1	2845S	Cell Signaling Technologies
PP2A-C	07-324	Millipore-Sigma
Methyl PP2A	05-577	Millipore-Sigma
Phospho PP2A	05-547	Millipore-Sigma
I1PP2A	sc-100767	Santa Cruz Biotechnology
I2PP2A		Dr. Prasad Lab
PP2A-B56	07-1221	Millipore-Sigma
PI3K-gamma	sc-166365	Santa Cruz Biotechnology
P62-SQSTM1	sc-28539	Santa Cruz Biotechnology
Phospho JNK1	07-175	Millipore-Sigma
Phospho ULK1-Ser757	14202	Cell Signaling Technologies
Phospho ULK1-Ser317	37762	cell Signaling Technologies
Phospho ULK1-Ser555	ABC124	millipore-Sigma
Phospho ULK1-Ser777	ABC213	Millipore-Sigma
ULK1	6439	Cell Signaling Technologies
Phospho TSC2	23402	Cell Signaling Technologies
TSC2	3635	Cell Signaling Technologies
Phospho p44/42 MAPK	4370S	Cell Signaling Technologies
P44/42 MAPK	4695S	Cell Signaling Technologies
Phospho P38 MAPK	4511S	Cell Signaling Technologies
P38 MAPK	9212S	Cell Signaling Technologies

Supplementary Table 2. Body weight and organ weights in female PI3KY^{-/-} and PI3KY^{+/+} mice

Female mice (saline)	PI3K ^{+/+} PF	PI3K ^{+/+} EF	PI3K ^{-/-} PF	PI3K ^{-/-} EF
Number	4	5	4	5
INITIAL BW	18.7±1.9	19.2±1.0	18.2±1.4	18.3±0.9
FINAL BW	22.8±2.2	22.3±0.6	22.4±1.4	20.9±1.2
Δ BW	4.1±0.5	3.2±0.9	4.2±1.9	2.6±0.9
Avg. intake (ml/d)	ND	23.4±2.8	ND	23.3±3.3
MUSCLE WT	0.22±0.01	0.16±0.04**	0.23±0.03	0.16±0.02**
HEART WT	0.12±0.01	0.12±0.01	0.12±0.02	0.10±0.01
LIVER WT	0.97±0.13	1.03±0.04	0.90±0.11	0.91±0.02
TG	43.0±11.8	69.6±37.2	45.0±6.7	68.5±7.6
ALT	22.7±9.1	35.8±8.3*	15.5±4.2	43.2±20.3*
AST	42.7±8.6	56.5±18.4	36.1±8.2	56.2±23.4
Female mice(colchicine)	PI3K ^{+/+} PF	PI3K ^{+/+} EF	PI3K ^{-/-} PF	PI3K ^{-/-} EF
Number	4	5	4	5
INITIAL BW	20.3±2.3	19.9±1.9	21.2±4.1	19.0±0.9
FINAL BW	24.2±1.4	23.9±1.4	22.9±2.5	22.0±1.2
Δ BW	3.9±1.1	4.0±1.1	1.7±1.9	2.6±0.9
Avg. intake (ml/d)	ND	23.4±3.2	ND	23.5±3.5
MUSCLE WT	0.23±0.02	0.16±0.02**	0.24±0.04	0.16±0.02***
HEART WT	0.16±0.03	0.14±0.01	0.16±0.02	0.14±0.01
LIVER WT	1.17±0.05	1.22±0.19	1.10±0.17	1.00±0.13
TG	58.8±22.6	65.6±13.1	59.9±20.6	76.5±23.2
ALT	26.2±9.4	33.8±6.0*	24.2±5.3	40.0±16.0**
AST	78.1±42.2	73.3±11.8	86.2±9.6	82.8±18.2

BW body weight in gm.; TG Hepatic triglyceride content (mg/g liver tissue); AST serum aspartate amino transferase (U/L); serum ALT alanine amino transferase (U/L). All values are mean±SD.

*** p<0.001, ** p<0.01, * p<0.05 vs. pair fed

Supplementary Figure Legends.

Supplementary Figure 1. Ethanol treatment does not alter myotube viability or PKB/Akt phosphorylation in myotubes and skeletal muscle from mice and human subjects.

A. Cell viability by trypan blue exclusion in myotubes treated with 100mM ethanol for different time points expressed as a percentage of control myotubes. **B.** Representative immunoblots of phosphorylated PKB/Akt Thr308 and Ser475 in myotubes treated with 100mM ethanol for the stated times (n=3 biological replicates), and skeletal muscle from pair or ethanol-fed mice (n=8 female mice in pair fed and n=10 in EF group) and human cirrhosis and controls (n=5 in each group). CIR cirrhosis patients; CTL control subjects; EF ethanol-fed mice; PF pair-fed mice, UnT untreated myotubes.

Supplementary Figure 2. Ethanol alters ULK1 phosphorylation in myotubes. Panel A.

Representative immunoblots and densitometry of phosphorylation of ULK1 from myotubes treated with 100 mM ethanol for different time points. **Panel B.** Representative immunoprecipitate of ULK1 immunoblotted for PP2A regulatory subunit, B56 in untreated or 100mM ethanol treated myotubes. N=3 biological replicates. Data expressed as mean±SD. ** p<0.01, ***p<0.001 vs. untreated myotubes. UnT untreated myotubes.

Supplementary Figure 3. Ethanol -induced signaling perturbations are mediated by TSC2 in myotubes and skeletal muscle from mice. Panel A.

Representative immunoblots and densitometry of total and phosphorylated TSC2^{Ser1462} in untreated or 100mM ethanol treated myotubes. **Panel B.** Representative immunoblots and densitometry of total and phosphorylated TSC2^{Ser1462} in gastrocnemius muscle from ethanol or pair-fed mice. **Panel C.** Representative immunoprecipitate of TSC2 immunoblotted for PP2A regulatory subunit, B56 in untreated or 100mM ethanol treated myotubes. **Panel D.** Representative immunoblots and densitometry of mTORC1 activation and signaling in untreated or 100mM ethanol for 6 h treated myotubes with stable knockdown of TSC2 or transfected with scrambled construct. Data expressed as mean±SD from blots from gastrocnemius muscle from n= mice in the pair-fed and n=6 mice from EF female mice in each arm and at least 3

biological replicates for myotubes treated with ethanol for different time points.. ** p<0.01, ***p<0.001 vs. muscle from pair-fed mice or untreated myotubes mice. E ethanol treated myotubes; EF Ethanol-fed mice; PF pair-fed mice; SCR scrambled construct; UnT untreated myotubes.

Supplementary Figure 4. Target specificity of ethanol-induced protein dephosphorylation in myotubes. Panel A. Representative immunoblots of phosphorylated and total ERK, p38 MAPK and JNK from untreated or 100mM ethanol treated myotubes. **Panel B.** Representative of immunoprecipitate of AKT immunoblotted for PP2A regulatory subunit, B56 in untreated or 100mM ethanol treated myotubes. Data and representative blots from at least 3 biological replicates for myotubes treated with 100mM ethanol for 6 h. E ethanol treated myotubes; UnT untreated myotubes.

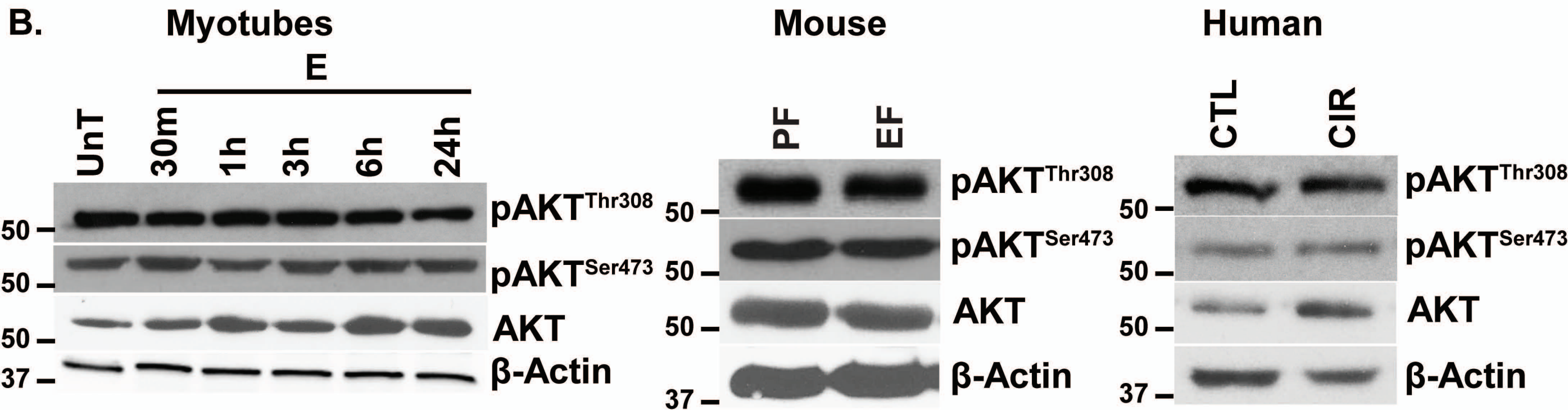
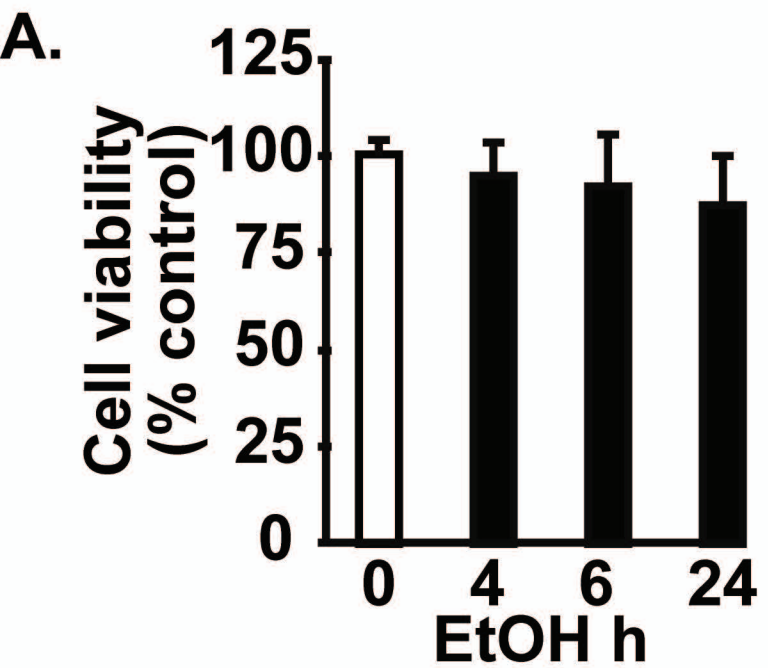
Supplementary Figure 5. Ethanol impairs I2PP2A binding to PP2A in skeletal muscle from mice and human subjects. Panel A-B. Immunoprecipitate of PP2A from the skeletal muscle from ethanol and pair-fed mice or human cirrhotics and controls immunoblotted for I1PP2A and I2PP2A. CIR cirrhosis patients; CTL control subjects; EF ethanol-fed mice; PF pair-fed mice.

Supplementary Figure 6. PI3KY dependent regulation of PP2A in myotubes and skeletal muscle from mice. Panel A. Representative immunoblots of PI3KY in untreated and 100mM ethanol for 6 h treated myotubes and in gastrocnemius muscle of pair-fed or ethanol-fed wild type C57Bl6 mice. **Panel B.** Representative immunoblots of mTORC1 signaling, phosphorylation of AMPK Thr¹⁷² and autophagy marker, LC3 lipidation in myotubes overexpressing PI3KY kinase dead construct. **Panel C.** PP2A activity in C2C12 myotubes overexpressing PI3KY kinase dead construct treated with or without 100mM ethanol for 6 h. **Panel D.** Representative immunoblots of mTORC1 signaling, phosphorylation of AMPK and LC3 lipidation in untreated or 100mM ethanol for 6 h treated myotubes stably overexpressing membrane targeted, myristoylated PI3KY. **Panel E.** PP2A activity from immunoprecipitates of AMPK and mTOR from myotubes stably overexpressing PI3KY either untreated or treated with 100mM ethanol for 6 h. Data and representative blots from at least 3 biological replicates for myotubes treated with 100mM ethanol for 6 h and gastrocnemius muscle from n=4 pair -

fed and n=6 ethanol-fed female mice in each group. Data expressed as mean±SD. ** p<0.01, ***p<0.001 vs. muscle from pair-fed (unpaired Student's 't' test) or untreated myotubes (ANOVA with Bonferroni post hoc). E ethanol treated; EF Ethanol-fed mice; PF pair-fed mice; KD kinase dead; MT membrane targeted myristoylated; SCR scrambled construct; UnT untreated myotubes.

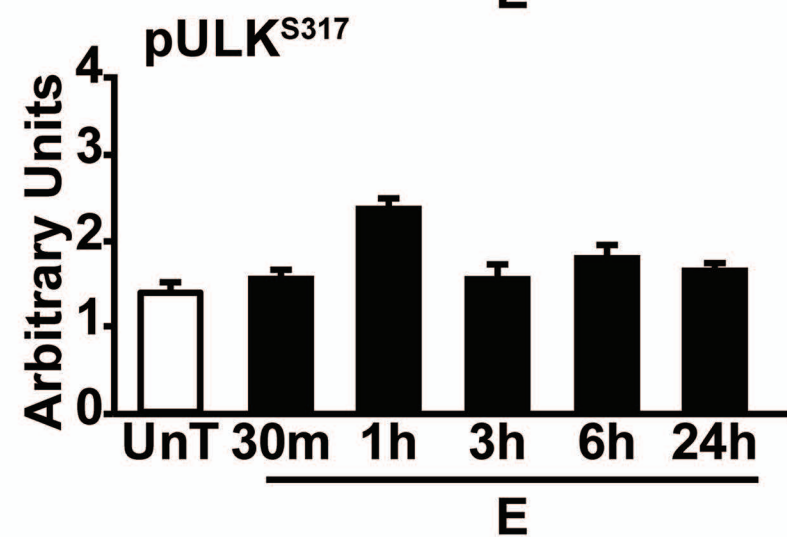
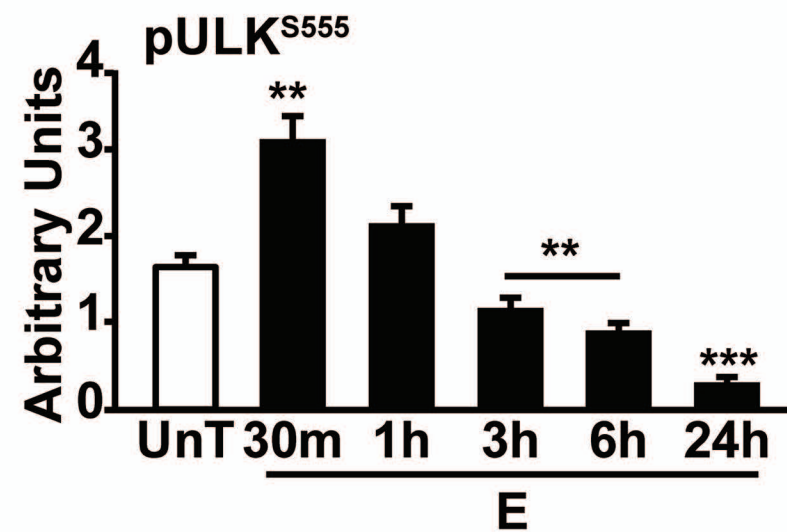
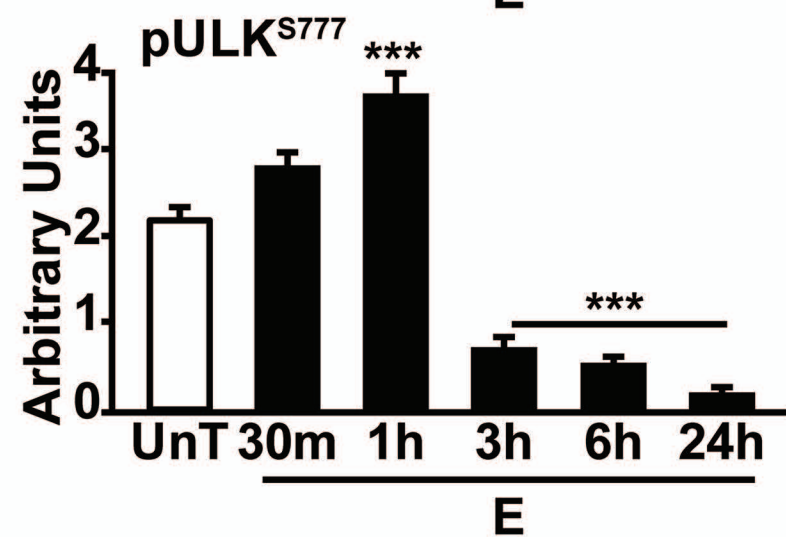
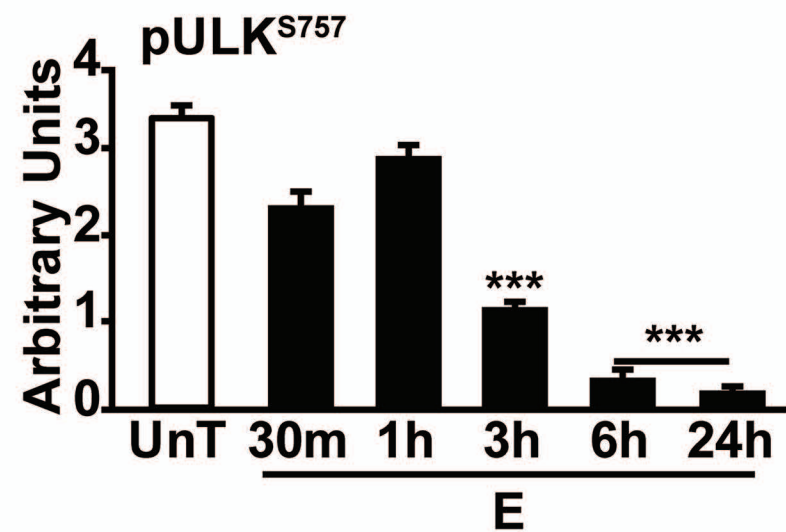
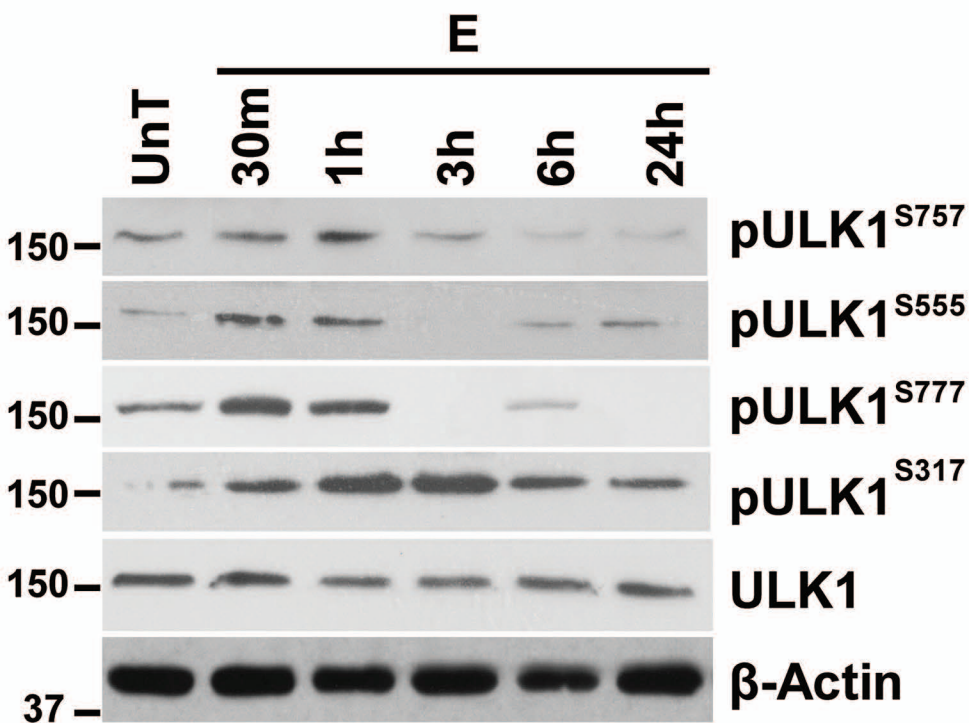
Supplementary Figure 7. Signaling responses and protein synthesis responses in ethanol-fed and pair-fed male PI3K^{+/+} and PI3K^{-/-} mice. Panel A. Representative immunoblots of phosphorylated AMPK and mTORC1 signaling and densitometry in muscle from ethanol and pair-fed PI3KY^{+/+} and PI3KY^{-/-} male mice. **Panel B.** Representative immunoblots of phosphorylated autophagy markers and densitometry in gastrocnemius muscle from ethanol and pair-fed PI3KY^{+/+} and PI3KY^{-/-} male mice. **Panel C.** Fractional and total muscle protein synthesis rates (FSR, TSR) in gastrocnemius muscle from ethanol and pair-fed PI3KY^{+/+} and PI3KY^{-/-} male mice. **Panel D.** Representative chromatogram and mass spectra of D5 phenylalanine in the bound fraction skeletal muscle from pair-fed (PF) and ethanol-fed (EF) mice. **Panel E.** PP2A activity gastrocnemius muscle of pair-fed or ethanol-fed PI3KY knockout female mice. Data expressed as mean±SD from gastrocnemius muscle from n=4 pair-fed and n=6 ethanol-fed mice. ** p<0.01; *** p<0.001.

Supplementary Figure 1

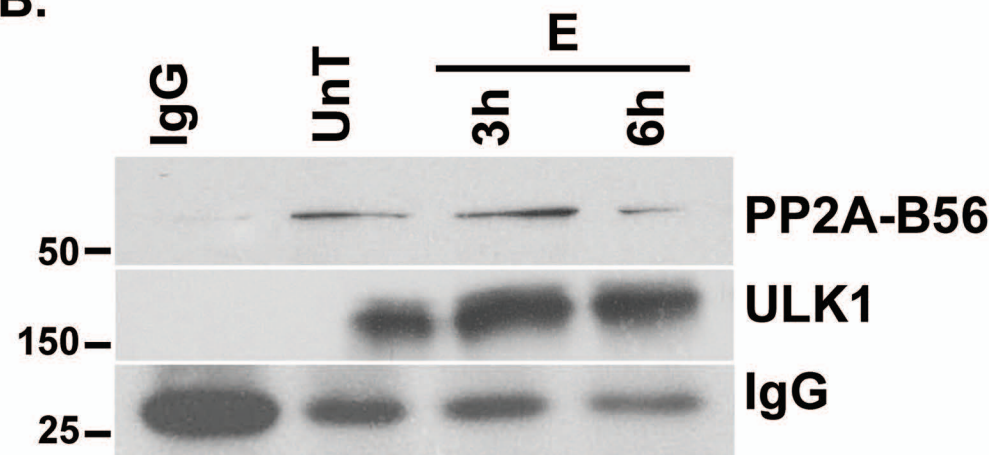


Supplementary Figure 2

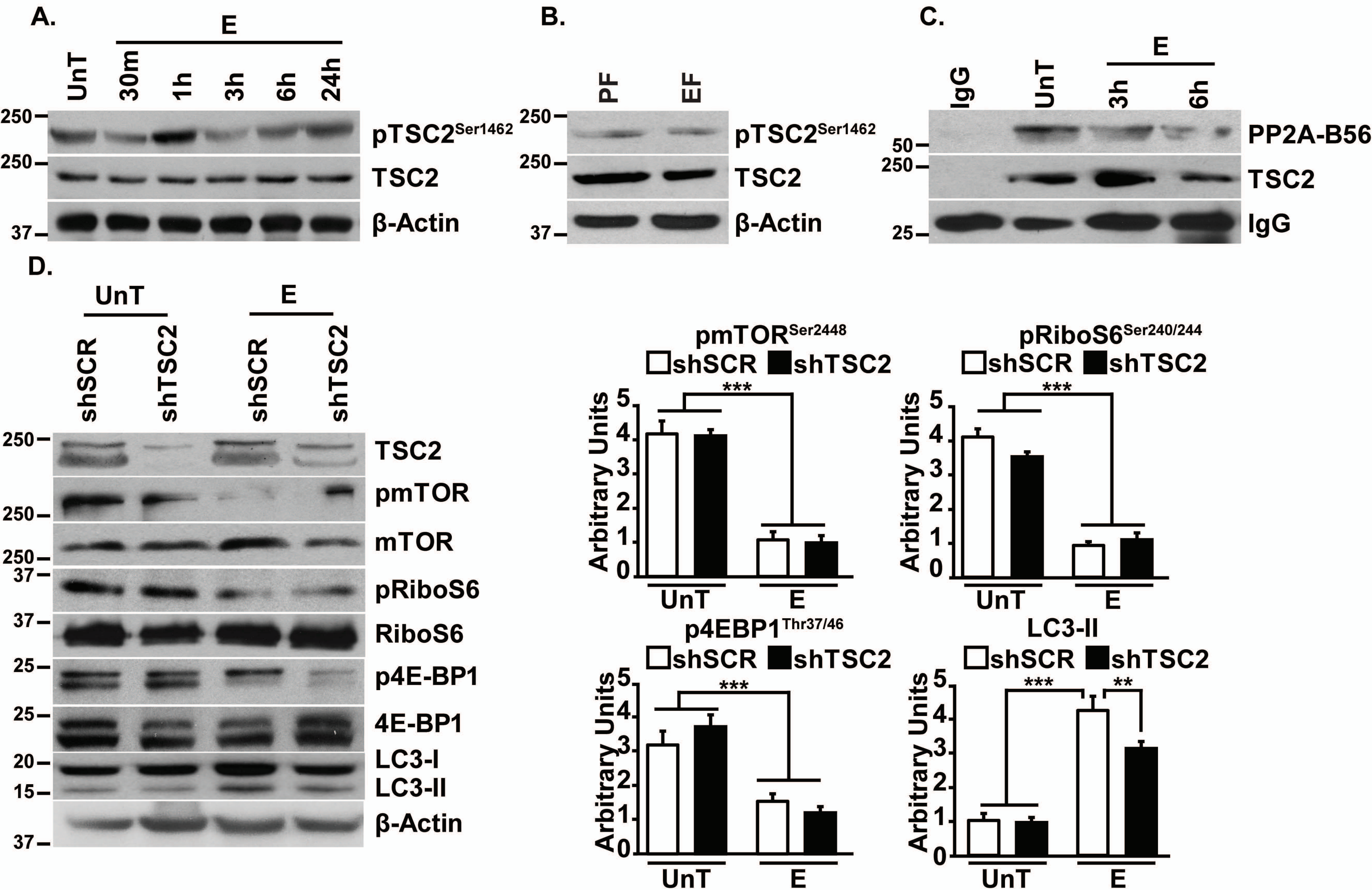
A.



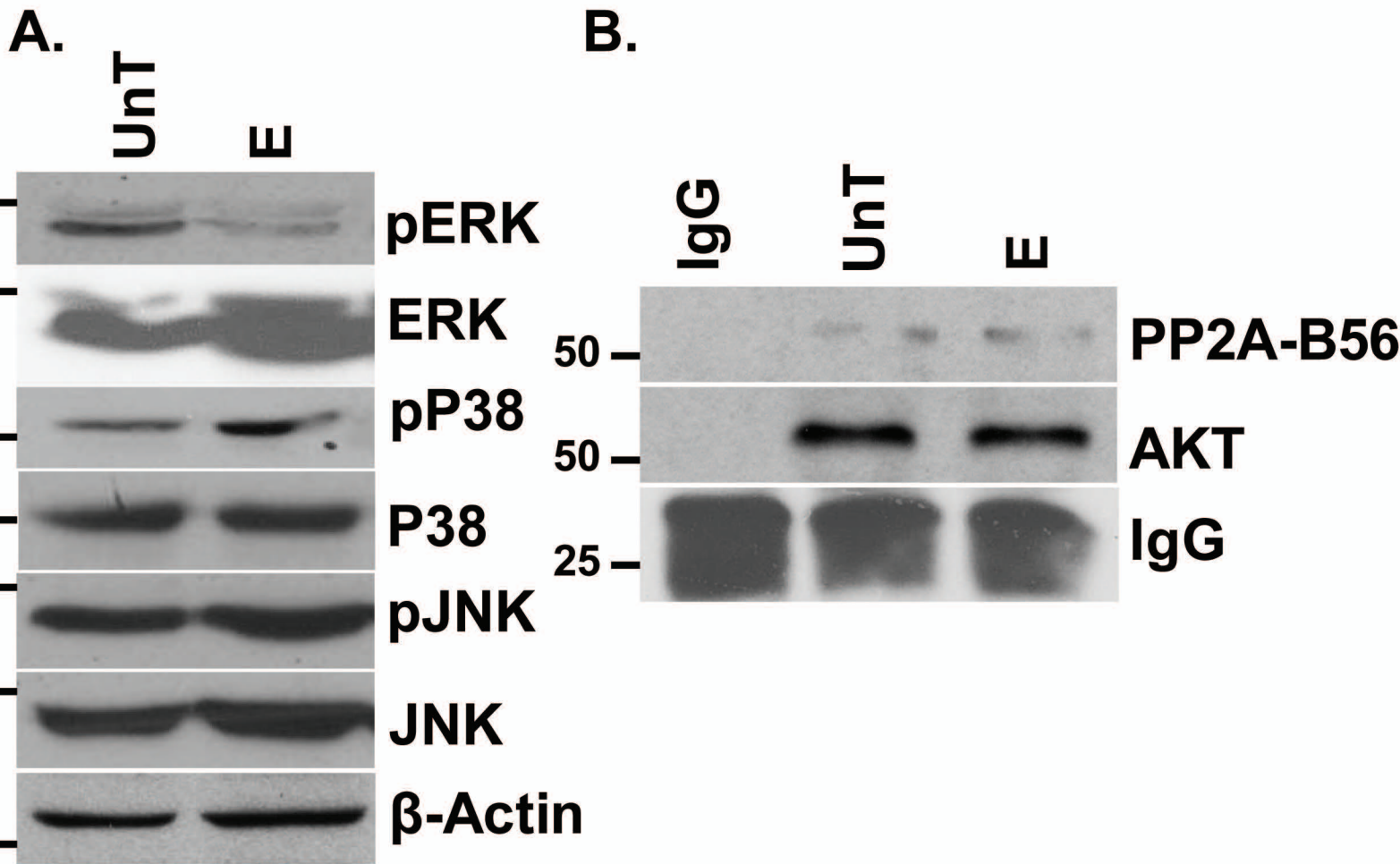
B.



Supplementary Figure 3

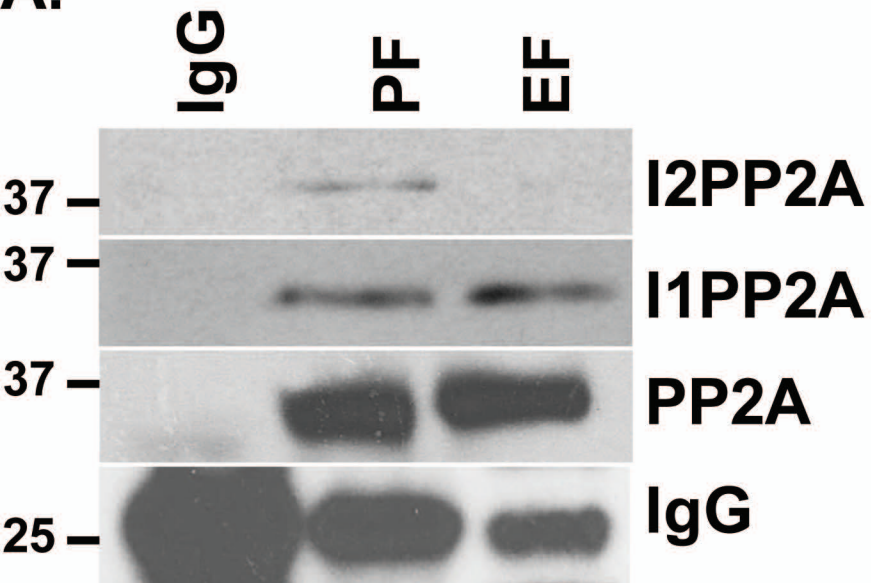


Supplementary Figure 4

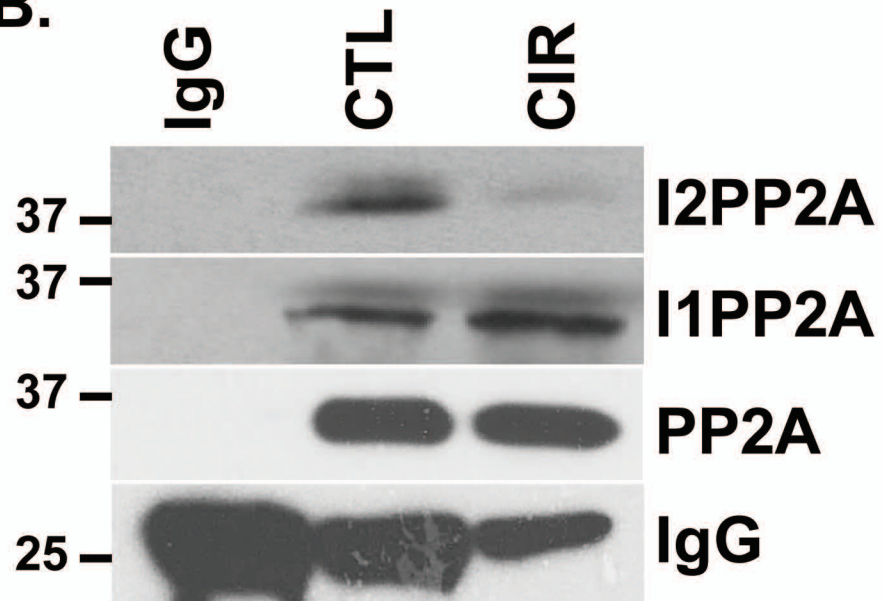


Supplementary Figure 5

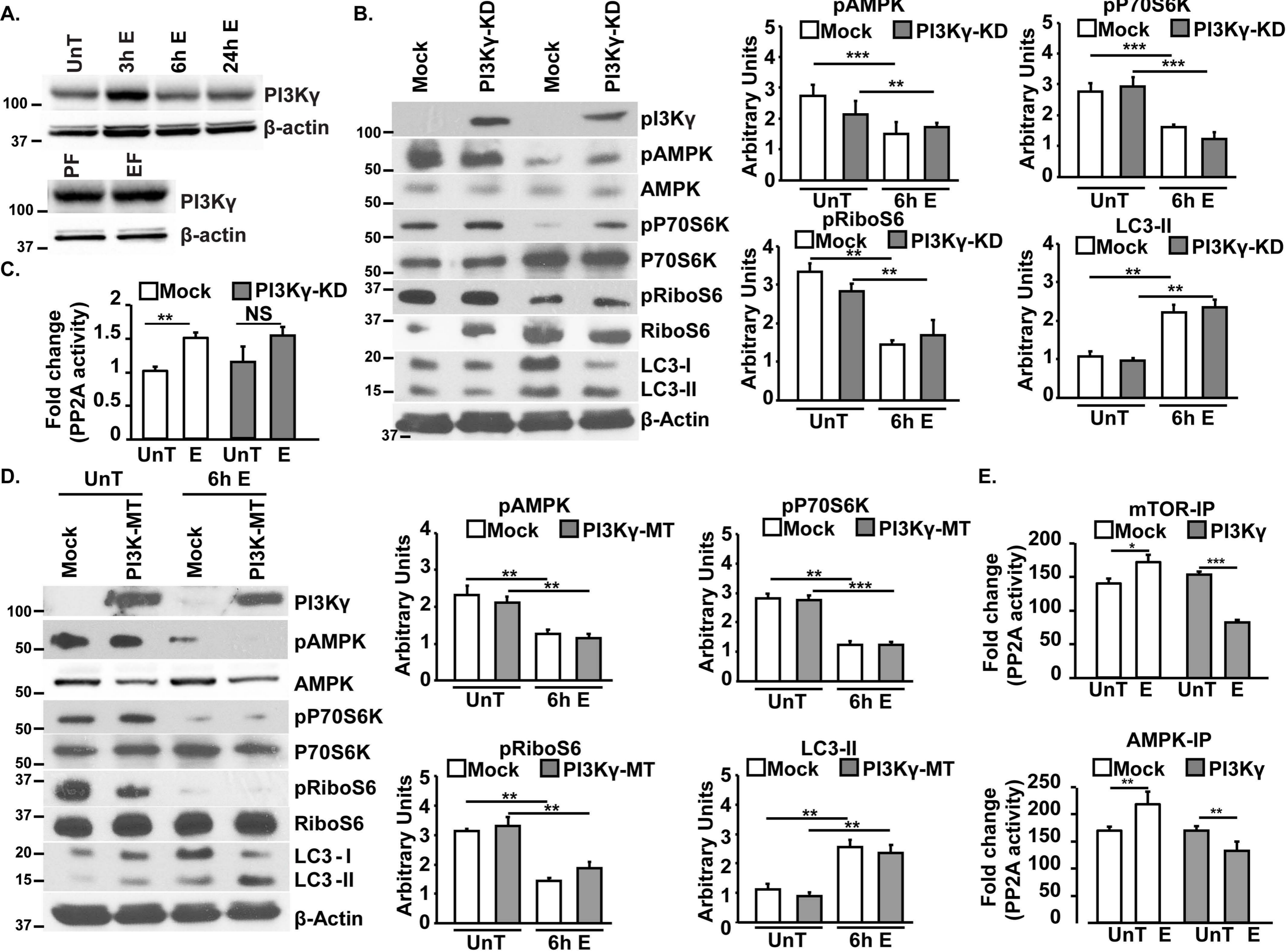
A.



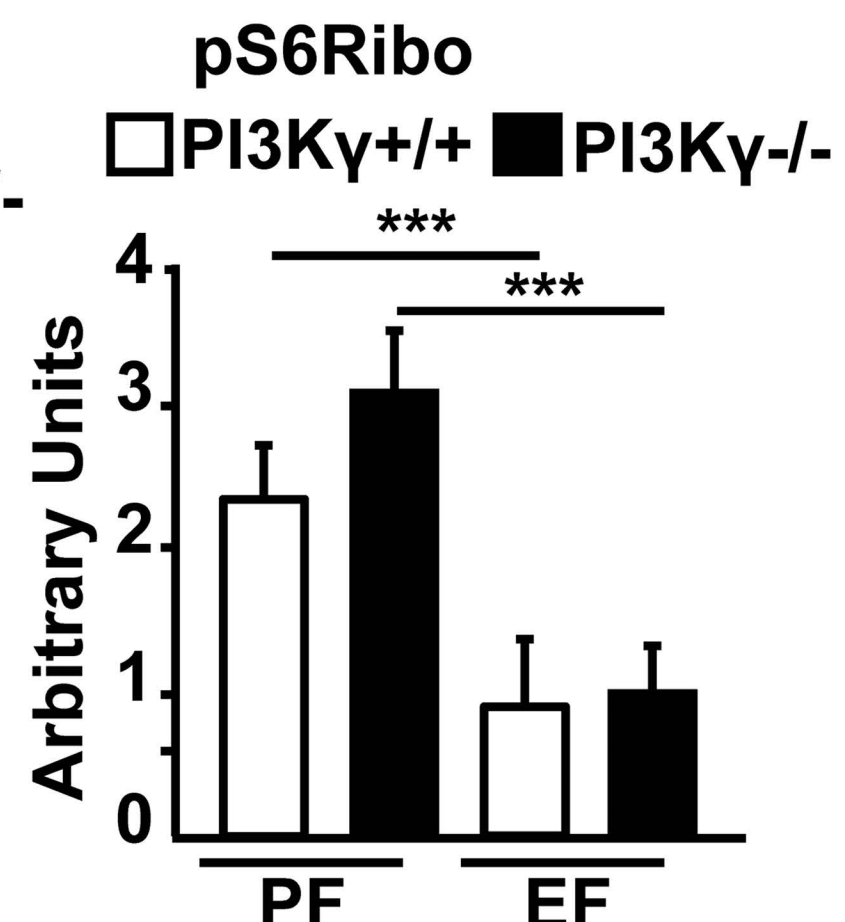
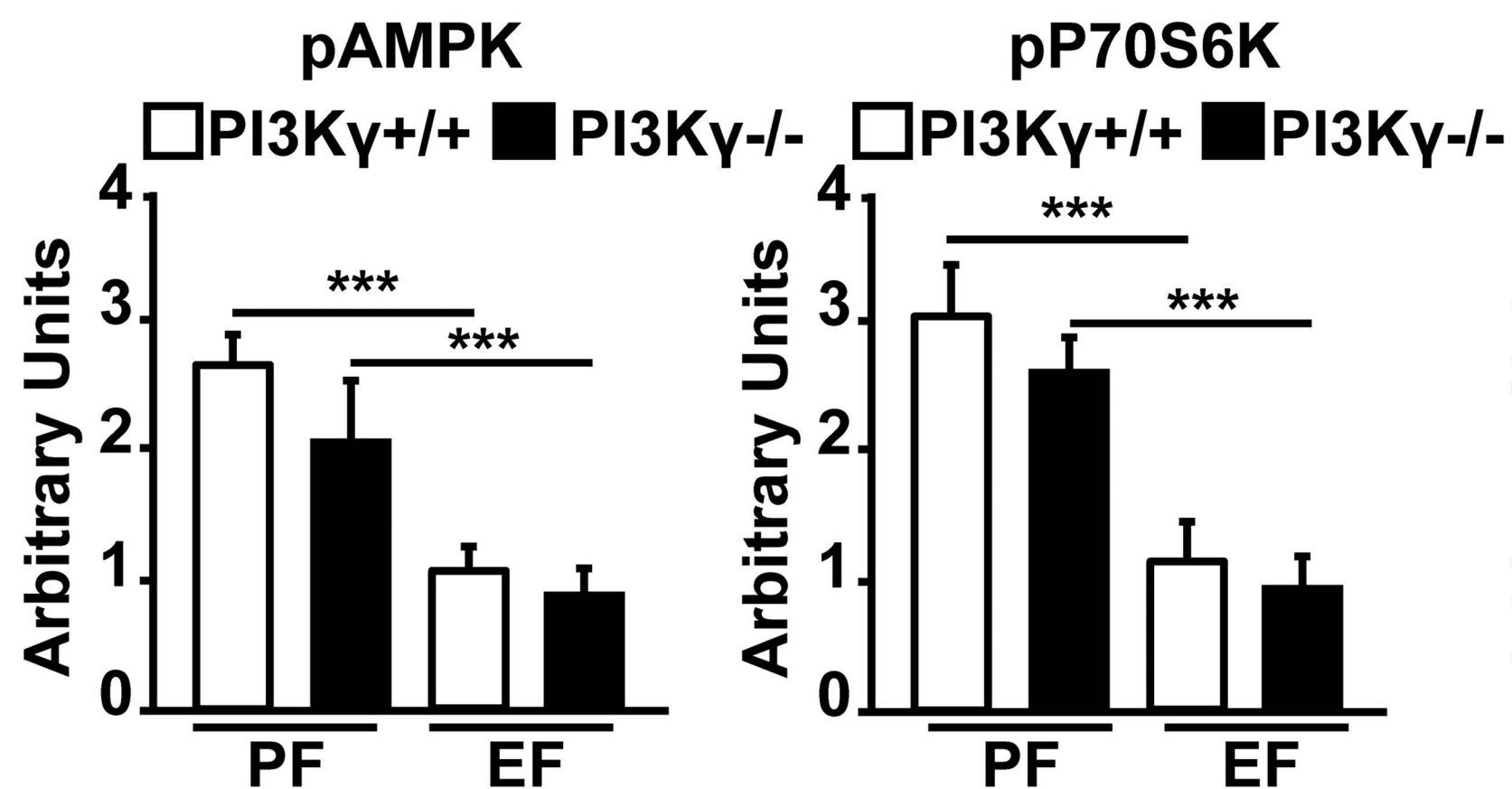
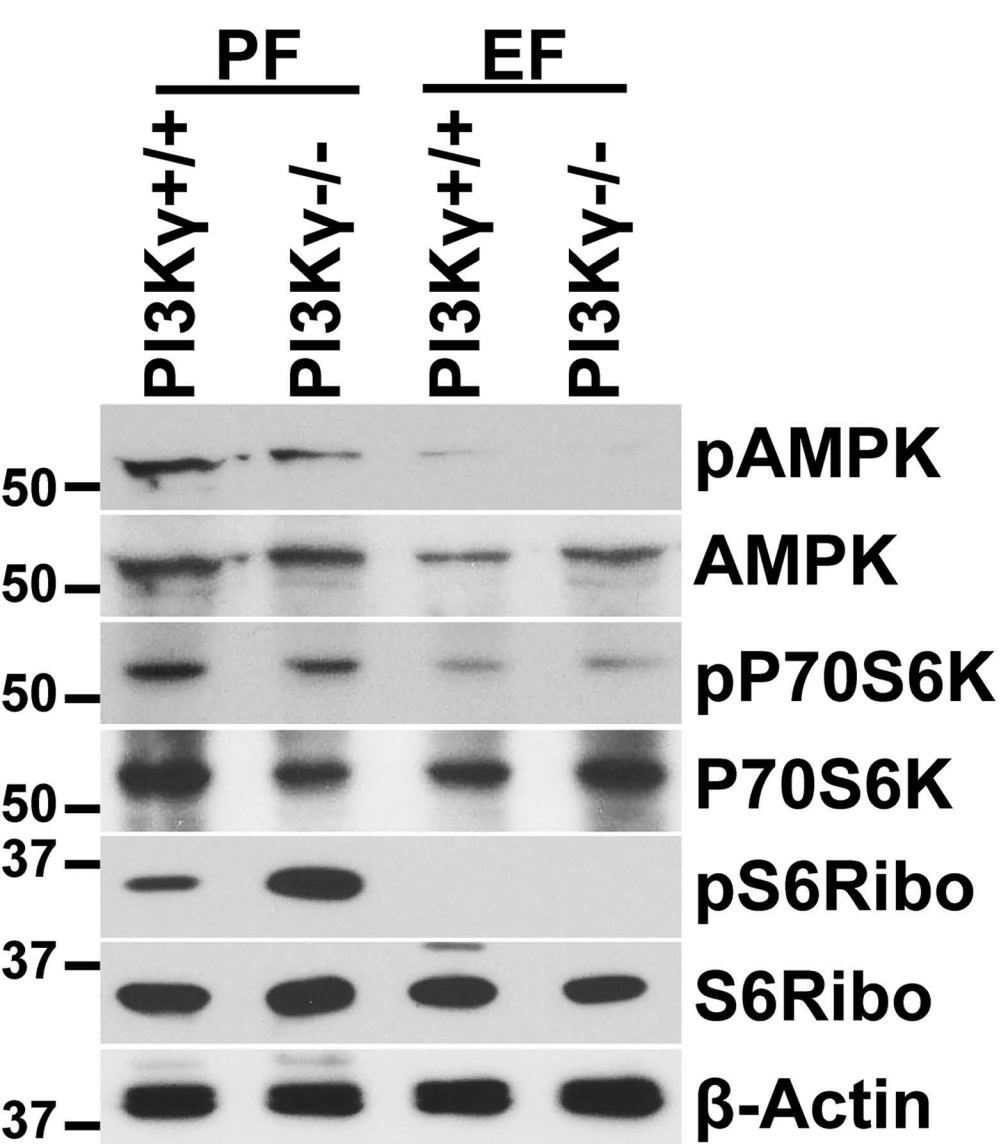
B.



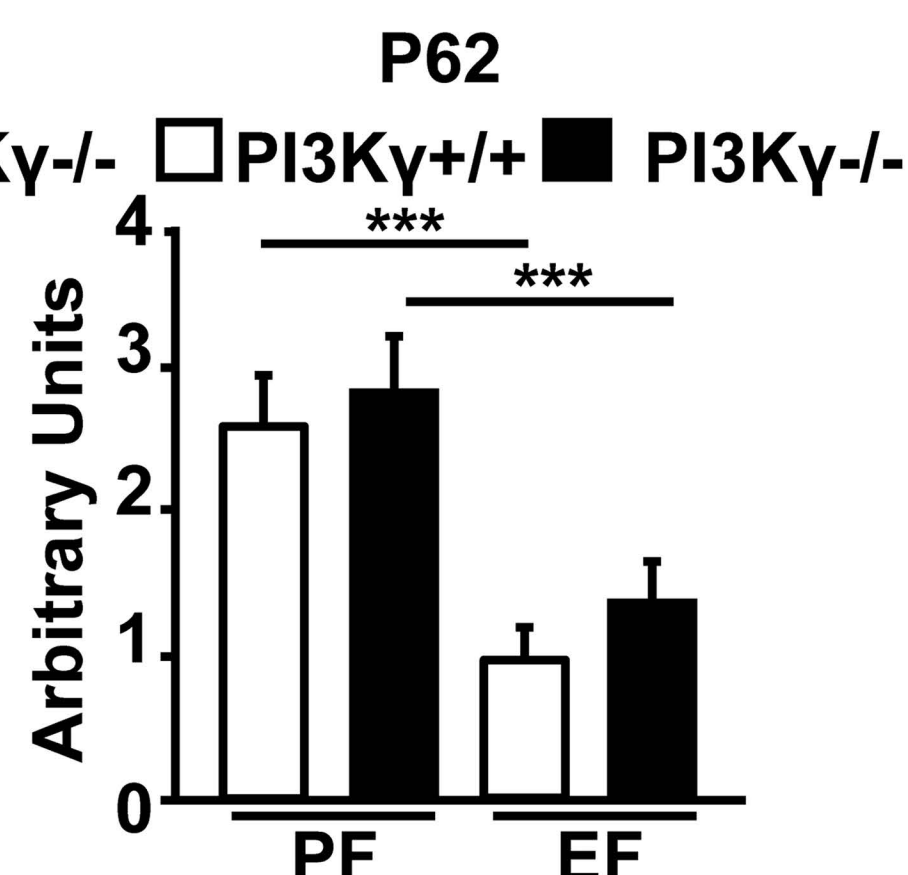
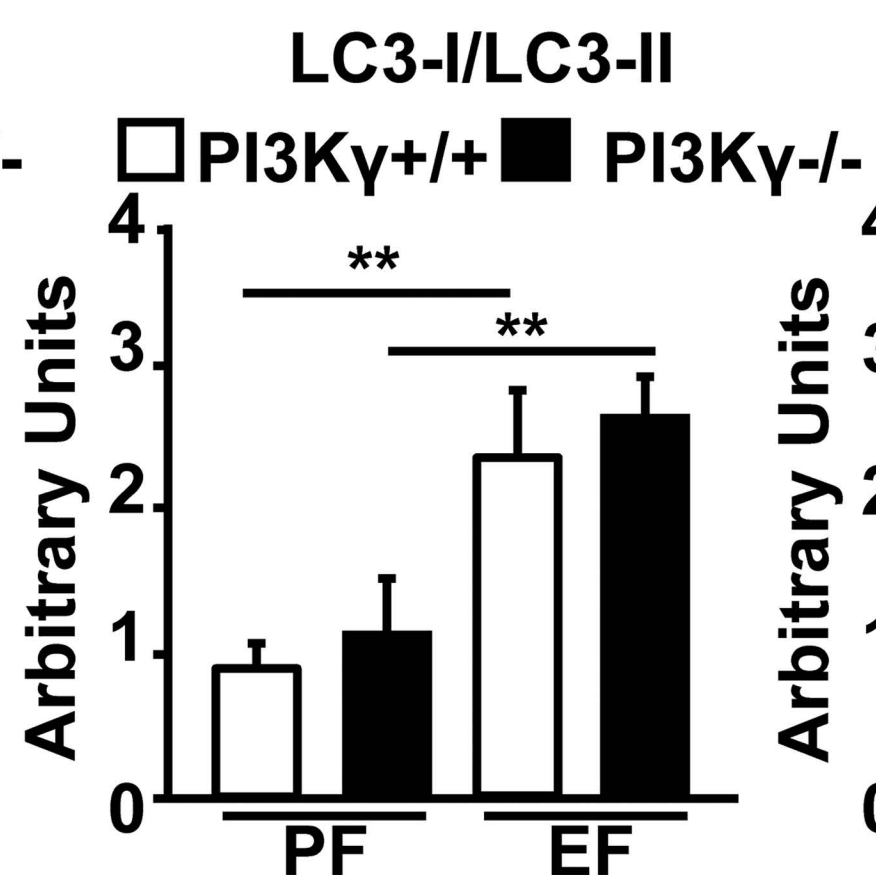
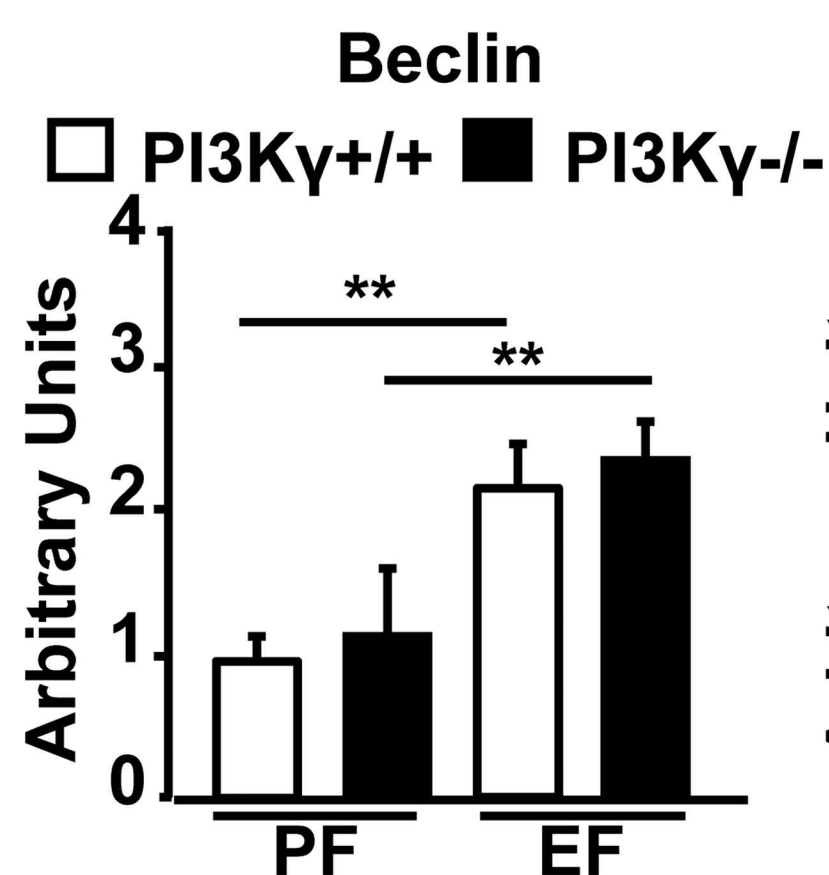
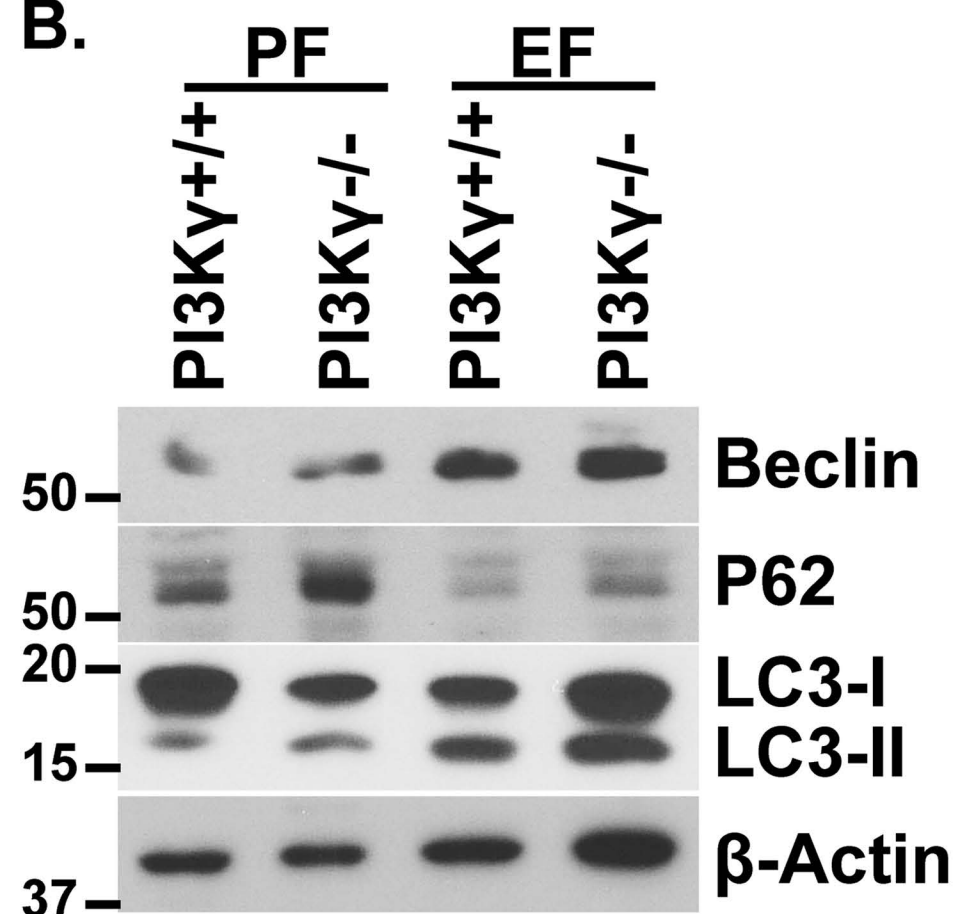
Supplementary Figure 6



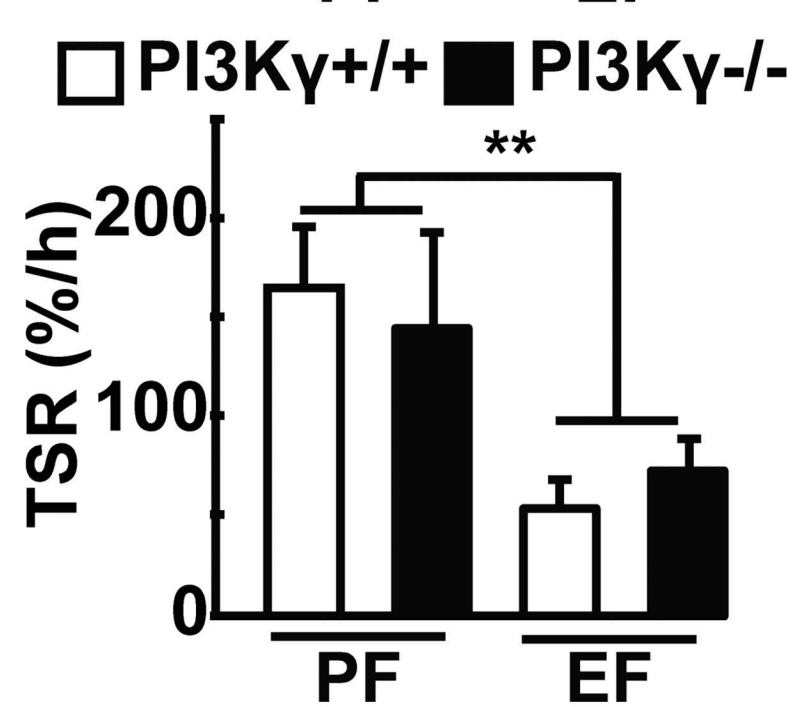
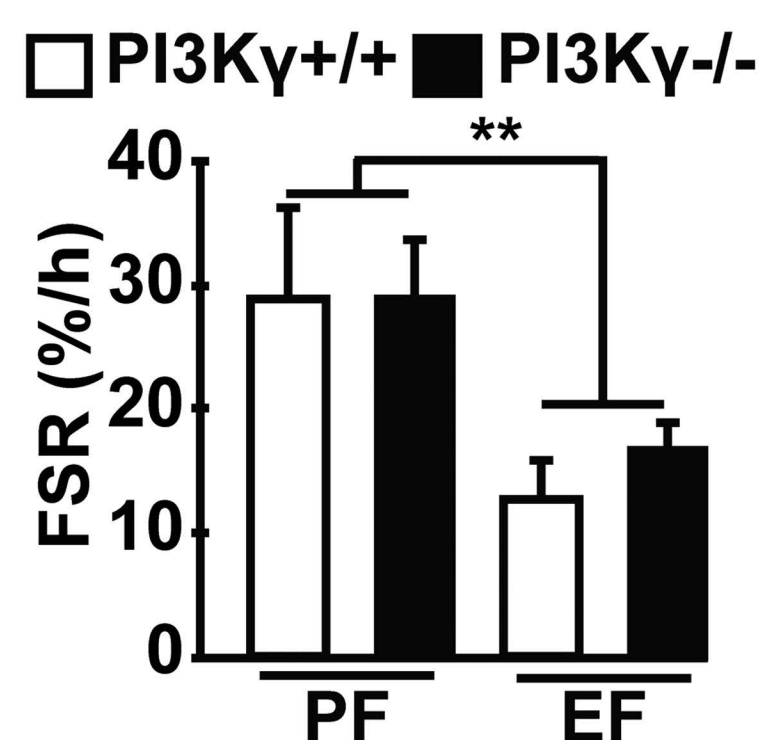
A.



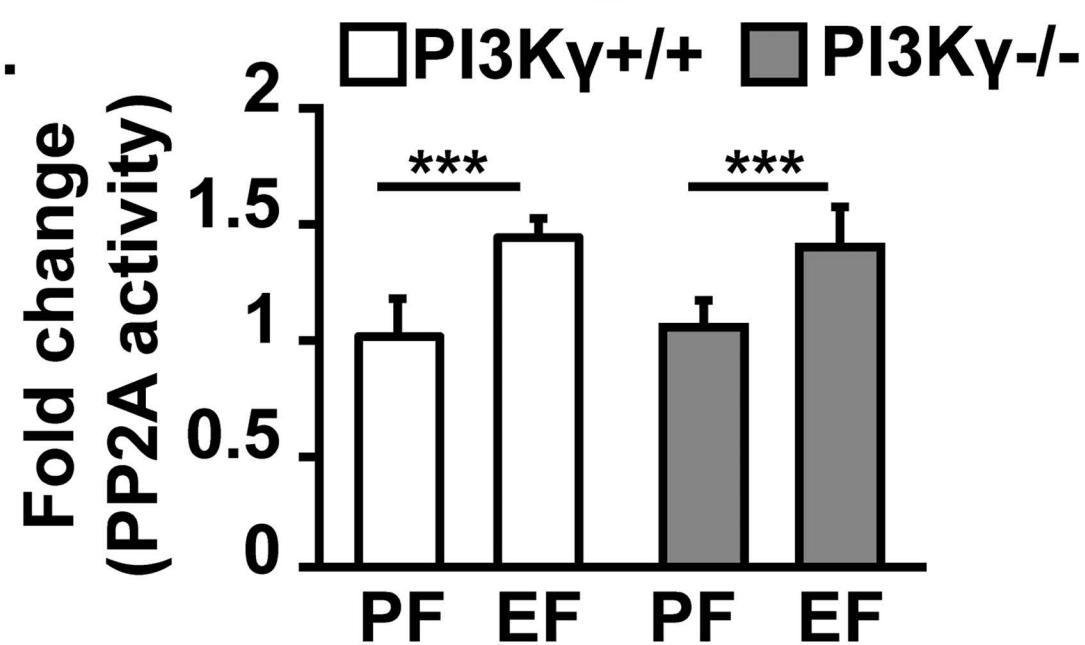
B.



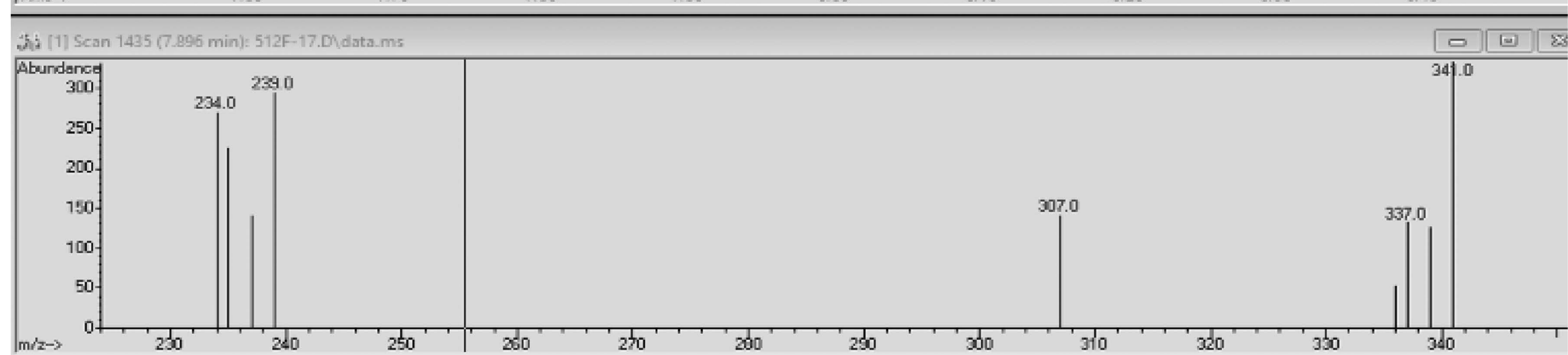
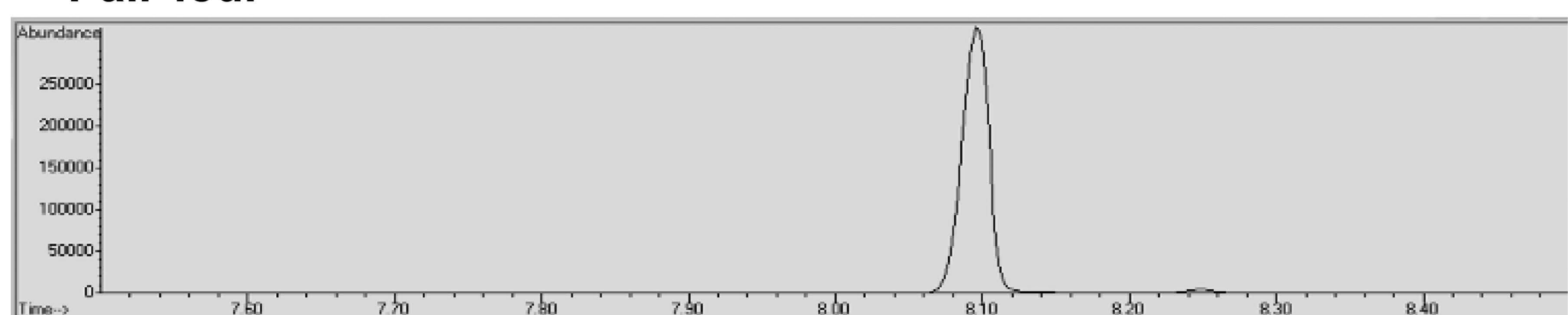
C.



E.



D. Pair-fed.



Ethanol-fed.

